Restricted Diffusion through Granular Materials

The restricted diffusion of nickel etioporphyrin is experimentally measured in six granular catalyst support materials. These materials include five γ-aluminas and one small-pore silica-alumina. Pore size distribution is narrow for three of the supports and roughly bimodal for the remaining three. Diffusivities are determined by a transient uptake technique utilizing a Freundlich equilibria adsorption isotherm.

Experimentally determined diffusivities agree well with restricted diffusion theory based on a circular pore model when the appropriate characteristic length scales are used to describe the molecule and pore size. For the restricted diffusion of dilute solute molecules in neutral pores, the appropriate measure of granular pore size is the hydraulic pore radius. Molecule size, in this case, is best described by a mean projected molecule radius for partitioning and a Stokes-Einstein radius for hydrodynamic aspects of restricted diffusion.

Kirk W. Limbach
James Wei
Department of Chemical Engineering
Massachusetts Institute of Technology
Cambridge, MA 02139

Introduction

Restricted diffusion occurs when molecular Brownian motion is significantly hindered by pore walls. Restrictive pores are typically of the same order-of-magnitude size as diffusing molecules. The diffusion of metal bearing compounds, such as asphaltenes and metalloporphyrins, in granular hydrotreating catalysts is restricted. Other important processes, in which restricted or hindered diffusion occurs, include membrane transport and size exclusion chromatography. Restricted diffusion has been reviewed by Deen (1987), and Anderson and Quinn (1974).

The theory of restricted diffusion of rigid spherical solutes in straight circular cylindrical pores has been exhaustively examined and experimentally verified (Deen, 1987). The restricted diffusion of nonspherical molecules in granular materials is less well understood, however, due to the complexities of molecule and pore shape. A better understanding of this type of diffusion would aid in the design of petroleum residue hydrotreating catalysts (Limbach and Wei, 1988).

Past researchers have sought to empirically model restricted diffusion in various types of porous materials (Satterfield et al., 1973; Baltus and Anderson, 1983; Chantong and Massoth, 1983). Empirical correlations are usually compared to theoretical predictions based on an equivalent circular cylindrical pore. The effects of molecule and pore shape, however, have not been systematically accounted for; therefore, a variety of characteristic length scales have been used to describe the molecule and pore size.

Satterfield et al. (1973) measured the diffusion of paraffins, aromatic hydrocarbons, and aqueous solutions of sugars in silica-alumina catalyst beads with a vary narrow pore size distribution. Diffusivities were correlated to λ_c, the ratio of the radius of the smallest circular cylinder through which the molecule could pass to the mean pore radius. The value of λ_c varied from roughly 0.1 to 0.5. Experimentally determined diffusivities for nonadsorbing solutes agree fairly well with the theory based on an equivalent λ_c circular pore at small λ_c. Experimental diffusivities are larger than those predicted by this theory at larger λ_c.

Baltus and Anderson (1983) measured the diffusion of asphaltenes in track-etched mica membranes with rhombus-shaped rectinlinear pores. Diffusion rates were correlated to λ_R, the ratio of the molecule Stokes-Einstein radius r_s to the radius of an equal area circular pore. A large range of molecule and pore sizes were tested and λ_R varied from roughly zero to just over unity. Baltus and Anderson compared their data to the theory based on an equivalent λ_R circular pore. Experimentally determined diffusivities were found to be substantially larger than this theory predicts at λ_R greater than 0.2.

Chantong and Massoth (1983) measured the diffusion of relatively rigid disc-like polyaromatic compounds including naphthalene, coronene, octaethylporphyrin, and tetraphenylporphyrin in alumina catalyst supports having a wide range of pore size distributions. Chantong and Massoth correlate their data to λ_a,

the ratio of the disc-like molecule radius to pore radius. Experiments were performed at λ_a less than 0.4. Molecule size was calculated from bond lengths and angles. The pore radius was calculated as twice the pore volume divided by the surface area. The data are compared with the theory based on an equivalent λ_a circular pore model. Experimental diffusivities agree fairly well with the theory.

In this study we analyze the effect of molecule and pore shape on restricted diffusion in granular materials and suggest characteristic length scales appropriate for this case. Previous results (Baltus and Anderson, 1983; Chantong and Massoth, 1983) are more accurately described by these length scales on an equivalent circular pore basis. Theoretical development is further substantiated by the experimental measurement of the restricted diffusion of nickel etioporphyrin in six catalyst support materials.

Theory

Effective diffusivity in granular materials, such as catalysts, may be described by

$$D_e = \frac{\epsilon D_\infty}{\tau} \cdot \frac{\Phi}{K} \tag{1}$$

where

ϵ = porosity
D_∞ = bulk diffusivity
τ = tortuosity
Φ = partition coefficient
K^{-1} = enhanced drag coefficient

The first part of Eq. 1 utilizes ϵ, D_∞, and τ to describe effective diffusivity in a tortuous material. This type of relation has been used for many years to describe nonrestricted diffusion in catalysts and is fairly well understood (Satterfield, 1980). The second part of Eq. 1 uses Φ and K^{-1} to include the effect of restricted diffusion. These variables have been used to describe restricted diffusion in rectilinear pores with good success, but little past work has been done to quantify restricted diffusion in tortuous materials. One of the primary goals in this study is to develop a method of estimating Φ and K^{-1} for tortuous granular materials such as hydrotreating catalysts.

Partitioning

The partition coefficient Φ is the equilibrium ratio of solute concentration within the interstitial space of a porous material to that in the bulk solution. For the case of a dilute solution in a neutral pore, Φ may be expressed as the ratio of orientation-averaged pore volume accessible to the molecule center to the total pore volume. Molecules immobilized on the pore wall would not diffuse along the pore and should not be included in Φ.

The partition coefficient of rigid nonspherical molecules may be expressed as the ratio of the configurational integrals:

$$\Phi = \frac{\int_x \int_\phi P(x, \phi)\, d^3x d^3\phi}{\int_x \int_\phi d^3x d^3\phi} \tag{2}$$

Integration is over the set of all molecule center positions $\underline{x}$ lying within the pore space, and all molecule orientations $\underline{\phi}$. The numerator of Eq. 2 represents the integration of the probability density, $P(\underline{x}, \underline{\phi})$, of the molecule having a given configuration $(\underline{x}, \underline{\phi})$. When any portion of the molecule does not lie within the pore space, the configuration is not allowed and $P(\underline{x}, \underline{\phi})$ is zero. The denominator is the corresponding integration over an identical configurational space, but evaluated for the bulk liquid where $P(\underline{x}, \underline{\phi})$ is, by definition, unity. The probability density, $P(\underline{x}, \underline{\phi})$, is a function of molecule and pore shape, size and molecule-pore interactions.

Unfortunately, no analytical solution exists for Eq. 2 for most cases of nonspherical molecules and complex pore networks, such as granular materials. As a consequence, Φ is typically estimated by assuming the molecule shape to be that of a sphere and the pore shape to be a circular cylinder. This approach is only valid, however, when the appropriate characteristic length scales are used to describe the molecule and pore size.

The appropriate characteristic molecule length to determine Φ is the mean projected molecule radius r_m, and the appropriate characteristic pore length is the pore hydraulic radius $(V/S)_p$.

For rigid axisymmetric molecules, the mean projected radius may be expressed as

$$r_m = \frac{1}{2} \int_0^\pi h \sin\theta \, d\theta \tag{3}$$

where h is the closest possible approach of the molecule center to a fixed flat surface (Baltus and Anderson, 1984). The approach h will vary with θ, the angle between the axis of rotation of the molecule and the surface's normal vector. The pore hydraulic radius $(V/S)_p$ is the ratio of the pore volume to pore surface area. For later convenience, λ_m is defined by

$$\lambda_m = r_m/(V/S)_p \tag{4}$$

Giddings et al. (1968) found that when Φ was plotted against λ_m, partitioning curves collapsed upon one another at small λ_m for several different molecule and inert rectilinear pore shapes.

Limbach et al. (1989) have analyzed the partitioning of axisymmetric molecules in neutral porous networks. Partitioning behavior in various-shaped rectilinear pores and tortuous materials, including sinusoidal pores and the interstitial space within fibrous and granular materials, was determined by Monte Carlo simulation. Granular materials were modeled as simple cubic (SC), body-centered cubic (BCC), and face-centered cubic (FCC) lattices of touching spherical grains. The void fraction of these lattices ranges from 0.26 for FCC to 0.48 for SC.

Figure 1 compares the partition coefficient for spherical molecules in these three lattice frameworks. The fact that partitioning in these lattices is not a strong function of void fraction is encouraging because it suggests that partitioning in granular materials might be estimated in practice by an equivalent rectilinear pore model. Even at appreciable values of λ_m, an equivalent circular pore represents these partitioning curves well, especially that of the FCC lattice.

The molecule cutoff size is a measure of the accessible pore diameter. Rigid molecules, which could fit in the body of a pore, will be excluded from passing through the throat of a pore when their smallest linear dimension exceeds the width of the throat. This point of exclusion is termed the molecule cutoff size.

Small molecule partitioning in granular materials may be

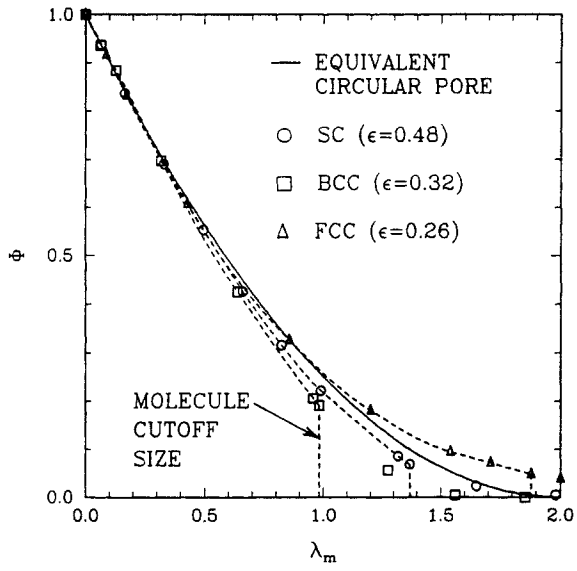

Figure 1. Comparison of spherical molecule partitioning in simple cubic (SC), body-centered cubic (BCC), and face-centered cubic (FCC) lattices of spherical grains.
From Limbach et al. (1989).

estimated from the circular pore model

$$\Phi = (1 - \lambda_m/2)^2 \tag{5}$$

if the void fraction and surface area are known. Large molecule partitioning can be estimated by Monte Carlo simulation or other more sophisticated techniques if the molecule cutoff size and particulars of grain morphology are known.

Hydrodynamic resistance

The enhanced drag coefficient K^{-1} is a measure of additional hydrodynamic resistance to the diffusion of a molecule in a porous material, as compared to that in bulk solution. In the absence of enhanced resistance ($K^{-1} = 1$), the diffusion rate of large spherical solutes moving at low Reynold's number conditions may be estimated from the Stokes-Einstein equation

$$D_\infty = \frac{kT}{6\pi\mu r_s} \tag{6}$$

where
k = Boltzmann's constant
T = temperature
μ = solvent viscosity
r_s = Stokes-Einstein radius of the solute molecule

The Stokes-Einstein radius may be used to characterize the size of any shape molecule when determining K^{-1} (Brenner, 1964). As in partitioning calculations, the pore size may be characterized by the hydraulic radius, $(V/S)_p$. For later convenience, λ_s is defined by

$$\lambda_s = r_s/(V/S)_p \tag{7}$$

When centerline approximations for rectilinear pores (Happel and Brenner, 1983) are compared on an equivalent λ_s basis, the solutions collapse upon one another at small λ_s. Nitsche (1989) has recently compared rectilinear pores of circular, slit and rhombic cross-section, and found that the asymptotic approximation of Brenner and Gaydos (1977) holds on an equivalent λ_s basis. The appropriate characteristic dimension to describe hydrodynamic resistance in granular materials is λ_s. The centerline approximation of Faxen (1922) for a spherical molecule in a neutral circular pore

$$K^{-1} = [1 - 1.0522\lambda_s + 0.2611\lambda_s^3 - 0.0296\lambda_s^5] \tag{8}$$

may be used to describe the enhanced drag coefficient K^{-1} for granular materials. Equation 8 provides a reasonable estimate of K^{-1} at small and intermediate λ_s, if the constrictive regions in the pores are consistent. Equation 8 does not take pore constrictions into account, however, and is therefore less accurate when the diffusing molecule size approaches that of the constricted regions of the pore.

Experimental Studies

Materials

In order to quantitatively model diffusion from experimental results, solute molecules and catalyst support materials must be well characterized. The diffusion rate of nickel etioporphyrin was measured in six catalyst support materials. Cyclohexane with a purity of 99% was used as a solvent for all transient uptake diffusion measurements and isotherms.

Nickel etioporphyrin, shown in Figure 2, was selected as a solute because it is representative of the metal-bearing compounds in crude oil. A major interest in this work is to simulate the diffusion of metal-bearing petroleum compounds in hydrotreating catalysts. Nickel etioporphyrin, which has been extensively characterized by Fleischer (1963), is a relatively rigid disc-like molecule.

The Stokes-Einstein radius r_s of nickel etioporphyrin was determined from the bulk diffusion rate to be 5.5 Å. The bulk diffusion rate was measured in a diaphragm-type diffusion cell.

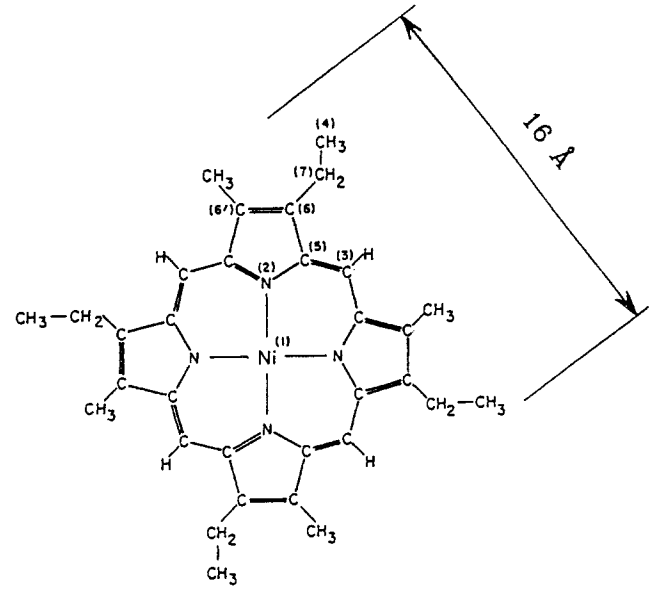

Figure 2. Structure of nickel etioporphyrin.
From Fleischer (1963).

Table 1. Results of Catalyst Support Characterization

Catalyst Support	*A*	*B*	*C*	*D*	*E*	*F*
Pore Diameter for All Pores Based on 4V/S,* Å	110	99	116	159	185	53
Micropore Diam. Pores Less than 500 Å, Å	107	97	116	120	129	33
Macropore Diam. Pores Greater than 500 Å, Å	1,600	1,700	N.A.	4,000	4,100	1,800
Pore Volume,** cm^3/g	0.728	0.620	0.636	1.074	1.187	0.560
Micropore Volume, %***	97.1	98.3	99.5	74.7	68.9	61.9
Macropore Volume, %***	2.9	1.7	0.5	25.3	31.1	38.1
Porosity†	0.703	0.667	0.679	0.770	0.796	0.605
Pellet Density, g/cm^3	0.965	1.076	1.068	0.717	0.671	1.080
Surface Area,‡ m^2/g	264	250	219	270	257	426
Micropore Surface Area, %***	99.8	99.9	100.0	99.0	98.6	98.9
Macropore Surface Area, %***	0.2	0.1	0.0	1.0	1.4	1.1

*Calculated from pore volume determined by nitrogen analysis and BET surface area.
**Determined by nitrogen analysis.
***Determined by mercury intrusion.
†Calculated from real support material density and support pellet density.
‡Determined by BET analysis.

A mean projected molecule radius r_m of 5.8 Å was estimated from Eq. 3, the experimentally determined r_s, and

$$r_s = a(1 - \gamma^2)^{1/2}[\sin^{-1}(1 - \gamma^2)^{1/2}]^{-1} \quad (9)$$

assuming a ratio of molecule length to diameter γ of 0.31. The molecule radius a was determined from Eq. 9 for use in Eq. 3. Equation 9, which is valid for oblate spheroids, was determined by Baltus and Anderson (1984) using the Stokes mobility coefficients of Happel and Brenner (1983).

The absence of solute aggregation was confirmed by determining that Beer's Law applies in the concentration range of interest (Dolphin, 1978).

Catalyst supports were characterized at the Unocal research facility in Brea, California, and Mobil Research and Development Corporation in Paulsboro, New Jersey. Characterization included nitrogen adsorption, nitrogen desorption, mercury intrusion, and catalyst density measurements. Results including the support pore volume, surface area, density, void fraction, and a simplified bimodal pore size distribution are summarized in Table 1. Six catalyst support materials, ranging in average pore size (measured by four times the pore volume divided by the surface area) from 53 to 185 Å, were used. Five of the support materials are constructed primarily of γ-alumina, and one support *F* is a silica-alumina. Catalyst support materials *A*, *B*, and *C* are essentially unimodal in pore size, while supports *D*, *E*, and *F* are roughly bimodal and contain some very large pores of up to roughly 10,000 Å in diameter.

Apparatus and Procedure

The diffusion of solute molecules into porous catalyst support pellets is measured using a transient uptake technique. This technique has been used for similar measurements by Satterfield et al. (1973), Prasher et al. (1977), Chantong and Massoth (1983), Guin et al. (1986), and Johnson et al. (1986). In the technique, solute is placed in a well-stirred batch system with a small quantity of catalyst support and a solvent carrier. The change in bulk solute concentration is measured as the solute diffuses into the support and is adsorbed on the pore walls. The diffusion rate may then be calculated from the rate of solute uptake, provided the equilibrium amount of solute adsorption on the catalyst support pore walls is known.

Equilibria adsorption isotherms describe the equilibrium amount of solute adsorbed on a catalyst support surface for a given concentration in solution. Equilibria adsorption isotherms were obtained by placing 25 mL of solution and between 0.01 and 0.05 g of catalyst support material in a 40-mL sample bottle, gently agitating the bottle in a constant temperature shaker bath at 30 + 1°C for two weeks, and then measuring the concentration of solute remaining in solution. The shaker bath was covered to prevent light from reaching the samples and altering concentration of nickel etioporphyrin. Fresh solution concentrations typically varied from 0.02 to 0.06 mg solute/mL.

Transient uptake diffusion experiments were conducted in the apparatus shown in Figure 3. The apparatus consists of a 400-mL glass vessel with teflon lined top. Stainless steel baskets hang from the top of the vessel to hold catalyst support particles. Temperature is measured by a thermocouple, and the vessel is agitated by a magnetic stir bar. Preliminary diffusion runs, in which the catalyst support particle radius was varied, indicate that a stirring speed of 800 rpm is sufficient for negligibly small mass transfer resistance at the particle surface. The stirring speed was maintained at 800 rpm. Samples were removed through a port in the top of the vessel with a clean, dry 1-mL pipette. The vessel is air-tight under normal operation.

A typical diffusion run consisted of loading the stainless steel baskets with 0.5 to 1.5 g of catalyst support. The baskets were then submerged in pure cyclohexane for 1 hour to allow the sol-

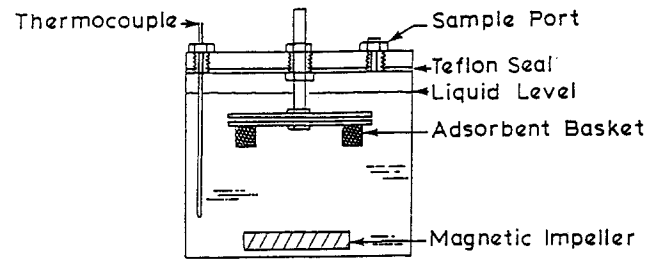

Figure 3. Transient uptake apparatus.

vent to permeate the support. A solution of roughly 0.01 to 0.03 mg solute/mL concentration was placed in the vessel and agitated. When the temperature of the vessel reached a steady 30 ± 1°C, the solution was sampled and the stainless steel baskets were lowered into the vessel. Samples were taken every 1 to 3 hours with a 1-mL pipette. A total of four to eight samples were taken per run. All experiments were conducted in a dry box to prevent water or other competitive adsorbents from entering the system. Solvents were dried with zeolite 4A prior to use.

Analysis of data

Diffusive flux within a catalyst support pellet may be described by Fick's second law, modified to account for solute adsorption. For a spherical catalyst pellet,

$$\epsilon \frac{\partial C}{\partial t} = D_e \left[\frac{\partial^2 C}{\partial r^2} + \frac{2}{r} \frac{\partial C}{\partial r} \right] - \rho_c \frac{\partial q}{\partial t} \tag{10}$$

where

$$C = 0 \quad \text{at} \quad t = 0$$

$$\frac{\partial C}{\partial r} = 0 \quad \text{at} \quad r = 0$$

$$C = C_R \quad \text{at} \quad r = R$$

and

$$-V_B \frac{\partial C_B}{\partial t} = A_E D_e \left[\frac{\partial C}{\partial r} \right]_{r=R} \tag{11}$$

where

C = solute concentration
r = radial coordinate of the catalyst pellet
D_e = effective diffusion coefficient
t = time
ϵ = support porosity
ρ_c = catalyst support density
q = equilibrium amount of solute adsorbed on the catalyst support surface
V_B = total volume of liquid solution
C_B = concentration of solute in the bulk phase
A_E = external surface area of catalyst support pellets
R = radius of the catalyst support pellets

A Freundlich isotherm,

$$q = A C^B \tag{12}$$

which has two adjustable constants, A and B, is used to describe the equilibria amount of solute adsorption on the catalyst.

The use of a nonlinear isotherm prohibits solving Eq. 10 analytically. A numerical shooting method utilizing a Crank-Nicholson finite difference scheme is used to solve Eq. 10, 11 and 12.

The approach to equilibrium f may be described by

$$f = (C_i - C)/(C_i - C_\infty) \tag{13}$$

where C_i is the initial solute concentration, and C_∞ is the equilibrium solute concentration after infinitely long contact of solution and catalyst support.

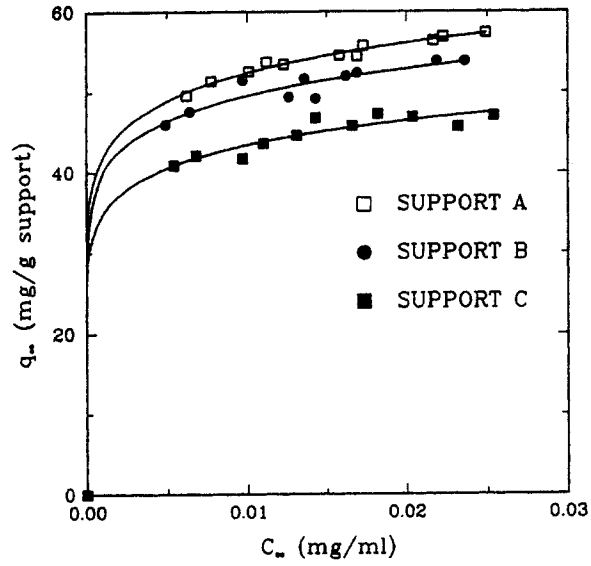

Figure 4. Equilibria adsorption isotherms for catalyst supports *A*, *B*, and *C*. Least squares fit of Freudlich isotherms are given as lines.

To determine D_e, f is experimentally measured as a function of time t, and a theoretical f is numerically calculated from Eq. 10, 11 and 12 as a function of the dimensionless time t_D.

$$t_D = D_e t / R^2 \tag{14}$$

The effective diffusivity may then be calculated from Eq. 14 by matching the experimental t to achieve a given f with the theoretical t_D to achieve that f. For additional accuracy, several matched values of t_D and t are obtained and plotted against each other. If the diffusion process has been accurately modeled, this plot yields a straight line. The effective diffusion coefficient D_e is calculated from the slope of the t_D vs. t line, adjusted to account

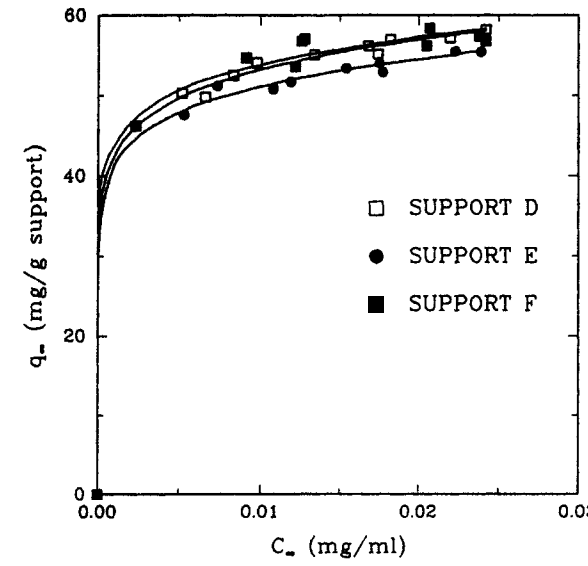

Figure 5. Equilibria adsorption isotherms for catalyst supports *D*, *E*, and *F*.
Least squares fit of Freundlich isotherms are given as lines.

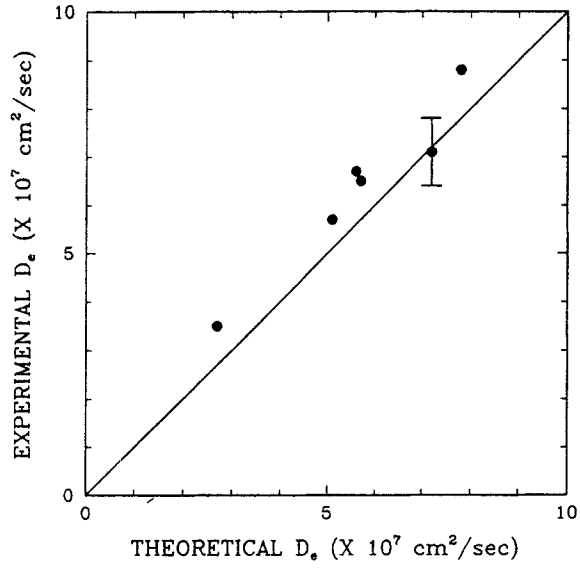

Figure 6. Experimental and theoretical diffusivities for six catalyst support materials.
Theoretical diffusivities assume a tortuosity of 4.0.

for the pellet size. The slope is determined by least squares analysis. A similar data analysis procedure was used by Chantong and Massoth (1983).

Results and Discussion

Equilibria adsorption isotherms

Equilibrium adsorption isotherm results for nickel etioporphyrin are given in Figures 4 and 5. Isotherms are plotted as final solution concentration vs. the equilibrium amount of solute adsorbed on the various catalyst support materials.

Least squares analysis was used to fit isotherm data points to Freundlich isotherms described by Eq. 14. Values of A and B are summarized in Table 2.

Effect of pore size on diffusivity

The effect of pore size distribution on experimentally measured diffusivities is in close agreement with circular pore theory on an equivalent λ_m and λ_s basis. Results are summarized in Table 3 and Figure 6.

Theoretically calculated diffusivities are determined *a priori* with no adjustable constants. Tortuosity, which is usually an adjustable constant, is taken to be four in this case and not adjusted to give the best fit to data. A tortuosity factor of four is recommended by Satterfield (1980) when the actual tortuosity is unknown. Pore size distribution was accounted for in experimentally measured diffusivities by the factor G_p. The correction factor G_p was determined assuming the bimodal pore size distribution described in Table 1 and a parallel pore model.

Table 3. Experimental and Theoretical Effective Diffusivities in Catalyst Support Materials

Catalyst Support Material	λ_m	λ_s	G_p^*	Experimental D_e^{**} $\times 10^7$ cm^2/s	Theoretical $D_e^{\dagger}$ $\times 10^7$ cm^2/s
A	0.21	0.20	0.98	6.5	5.7
B	0.23	0.22	0.98	5.7	5.1
C	0.20	0.19	1.0	6.7	5.6
D	0.15	0.14	0.77	7.1	7.2
E	0.13	0.12	0.72	8.8	7.8
F	0.44	0.42	0.88	3.5	2.7

*Pore-size distribution is accounted for by a parallel pore model.
**Corrected for pore-size distribution.
†Calculated assuming a tortuosity of 4.

Theoretical effective diffusivities are calculated for each of the six catalyst support materials used in this study from Eq. 1. The bulk diffusion rate D_∞ was determined experimentally in a diaphragm-type diffusion cell. The porosity ϵ of each support was determined from density measurements of pure and pelletized materials. The partition coefficient Φ was calculated from the λ_m in Table 3 using Eq. 4. The enhanced drag coefficient K^{-1} was calculated from the λ_s shown in Table 3 using Eq. 8. Equation 8 agrees quite well with the more rigorous work of Bungay and Brenner (1973) at λ_s less than 0.8.

Solute adsorption on the pore walls could theoretically lower the experimentally determined effective diffusivities by as much as 6% with monolayer coverage. This effect, however, was not accounted for, because the extent of adsorptive interference cannot be experimentally measured.

Data precision was determined from experimental runs for catalyst support D. An error bar representative of a 95% confidence interval is shown in Figure 6. The diffusion rate of nickel etioporphyrin in catalyst support D is determined with 95% confidence to be within 9.5% of the experimentally-determined mean.

Conclusions

In granular materials, such as some heterogeneous catalysts, the theory of restricted diffusion is complicated by the tortuous nature of the pores. Past researchers have used various characteristic length scales to describe how the molecule and pore size relate to experimentally measured restricted diffusivities (Satterfield et al., 1973; Baltus and Anderson, 1983; Chantong and Massoth, 1983). None of these researchers has suggested the use of both λ_m for partitioning and λ_s for hydrodynamic calculations. If these appropriate length scales are used, the complex problem of restricted diffusion in granular materials can sometimes be represented by the much simpler case of a circular cylindrical pore. A straightforward approach to calculate restricted diffusion in granular materials similar to hydrotreating catalysts is developed in this study. The approach is based on an

Table 2. Experimentally Determined Freundlich Isotherm Parameters

Catalyst Support Parameters	*A*	*B*	*C*	*D*	*E*	*F*
A	82.3	76.6	68.1	83.9	78.5	81.7
B	0.0979	0.0944	0.0976	0.0988	0.0931	0.0905

equivalent λ_m and λ_s circular pore model and is experimentally confirmed.

The close agreement of experimentally-determined and theoretically-calculated diffusion rates indicates that the effects of surface diffusion and solute concentration are minimal in this system.

Notation

a = radius of axisymmetric molecule
A = preexponential factor or Freundlich isotherm constant
A_E = external surface area of catalyst support
b = half axial length of axisymmetric molecule
B = Freundlich isotherm constant
C = concentration of solute
C_B = concentration of solute in bulk phase
C_i = initial concentration of solute before adsorption occurs
C_R = concentration of solute or reactant at $r = R$
C_∞ = solute concentration at equilibrium
D_e = effective diffusivity
D_∞ = diffusivity in dilute bulk solution
E = interaction energy between solute molecule and pore wall
f = approach to equilibrium uptake defined by Eq. 13
G_p = correction factor for parallel pores of a given size distribution
h = closest approach of a molecule center to a flat surface at a given molecule orientation
k = Boltzmann's constant
K^{-1} = enhanced drag coefficient
$P(\underline{x}, \underline{\phi})$ = probability density of the molecule having configuration $(\underline{x}, \underline{\phi})$
q = equilibrium uptakes of solute on catalyst support surface
r = radial coordinate in catalyst support pellet
R = catalyst support radius
r_m = mean projected radius of molecule
r_s = Stokes-Einstein radius of diffusing molecule
S = surface area of catalyst support
t = time
T = absolute temperature
t_D = dimensionless contact time of catalyst support material and solution as defined by Eq. 14
V = pore volume
V_B = volume of solution in transient uptake vessel
$(V/S)_p$ = hydraulic radius of porous medium, the ratio of pore volume to surface area
x = position of molecule center

Greek letters

ϵ = catalyst or catalyst support porosity
γ = molecule aspect ratio, b/a
θ = polar angle between pore and molecule axes
λ_a = ratio of molecule size to circular pore radius, a/r_p
λ_b = ratio of molecule size to circular pore radius, b/r_p
λ_c = ratio of the smallest circle through which the molecule can pass to the mean pore radius
λ_m = ratio of molecule to pore size expressed as $r_m/(V/S)_p$
λ_R = ratio of molecule r_s to the radius of an equal area circular pore
λ_s = ratio of molecule to pore size expressed as $r_s/(V/S)_p$
μ = solvent viscosity
ϕ = azimuthal angle specifying molecule orientation
$\underline{\phi}$ = set of angles describing molecule orientation
Φ = partition coefficient
ρ_c = catalyst or catalyst support density
τ = catalyst tortuosity

Literature Cited

Anderson, J. L., and J. A. Quinn, "Restricted Transport in Small Pores: A Model for Steric Exclusion and Hindered Particle Motion," *Biophys. J.*, **14,** 130 (1974).

Baltus, R. E., and J. L. Anderson, "Hindered Diffusion of Asphaltenes Through Microporous Membranes," *Chem. Eng. Sci.*, **38,** 1959 (1983).

———, "Comparison of G.P.C. Elution Characteristics and Diffusion Coefficients of Asphaltenes," *Fuel*, **63,** 530 (1984).

Brenner, H., "Effect of Finite Boundaries on the Stokes Resistance of an Arbitrary Particle: Part 2 Asymmetrical Orientations," *J. Fluid Mech.*, **18,** 144 (1964).

Brenner, H., and L. J. Gaydos, "The Constrained Brownian Movement of Spherical Particles in Cylindrical Pores of Comparable Radius," *J. Colloid Interf. Sci.*, **58,** 312 (1977).

Bungay, P. M., and H. Brenner, "The Motion of a Closely-Fitting Sphere in a Fluid-Filled Tube," *Int. J. Multiphase Flow*, **1,** 25 (1973).

Chantong, A., and F. E. Massoth, "Restrictive Diffusion in Aluminas," *AIChE J.*, **29,** 725 (1983).

Deen, W. M., "Hindered Transport of Large Molecules in Liquid-Filled Pores," *AIChE J.*, **33,** 1409 (1987).

Dolphin, D., ed., *The Porphyrins*, Vols. 1–7, Academic Press, New York (1978).

Fleischer, E. B., "The Structure of Nickel Etioporphyrin: I," *J. Amer. Chem. Soc.*, **85,** 146 (1963).

Ghai, R. K., H. Ertl, and F. A. L. Dullien, "Liquid Diffusion of Nonelectrolytes: Part 1," *AIChE J.*, **19,** 881 (1973).

Giddings, J. C., E. Kucera, C. P. Russell, and M. N. Myers, "Statistical Theory for the Equilibrium Distribution of Rigid Molecules in Inert Porous Networks: Exclusion Chromatography," *J. Phys. Chem.*, **72,** 4397 (1968).

Guin, J. A., K. J. Tsai, and C. W. Curtis, "Intraparticle Diffusivity Reduction During Hydrotreatment of Coal-Derived Liquids," *Ind. Eng. Chem. Proc. Des. Dev.*, **25,** 515 (1986).

Happel, J., and H. Brenner, *Low Reynolds Number Hydrodynamics*, Nijhoff, The Hague (1983).

Johnson, B. G., F. E. Massoth, and J. Bartholdy, "Diffusion and Catalytic Activity Studies on Resid-Deactivated HDS Catalysts," *AIChE J.*, **32,** 1980 (1986).

Limbach, K. W., J. M. Nitsche, and J. Wei, "Partitioning of Nonspherical Molecules between Bulk Solution and Porous Solids," *AIChE J.*, **35,** 42 (1989).

Limbach, K. W., and J. Wei, "Effect of Nonuniform Activity on Hydrodemetallation Catalyst," *AIChE J.*, **34,** 305 (1988).

Nitsche, J. M., "Effective Transport of Spherical and Nonspherical Brownian Particles within Heterogeneous Media," PhD Thesis, Massachusetts Institute of Technology (1989).

Prasher, B. D., G. A. Gabriel, and Y. H. Ma, "Catalyst Deactivation by Pore Structure Changes: The Effect of Coke and Metal Depositions on Diffusion Parameters," *Ind. Eng. Chem. Proc. Des. Dev.*, **17,** 266 (1977).

Satterfield, C. N., *Heterogeneous Catalysis in Practice*, McGraw-Hill, New York (1980).

Satterfield, C. N., C. K. Colton, and W. H. Pitcher, "Restricted Diffusion in Liquids within Fine Pores," *AIChE J.*, **19,** 628 (1973).

Reid, R., J. M. Prausnitz, and T. K. Sherwood, *The properties of Gases and Liquids, 3rd ed.*, McGraw-Hill, New York (1977).

Manuscript received July 18, 1989, and revision received Nov. 27, 1989.